A New Generation of the IMAGIC Image Processing System

MARIN VAN HEEL, GEORGE HARAUZ,[1] AND ELENA V. ORLOVA

Fritz Haber Institute of the Max Planck Society, Faradayweg 4-6, D-14195 Berlin, Germany

RALF SCHMIDT

Fritz Haber Institute of the Max Planck Society, Faradayweg 4-6, D-14195 Berlin, Germany; and Image Science Software GmbH, Mecklenburgische Strasse 27, D-14197 Berlin, Germany

AND

MICHAEL SCHATZ

Image Science Software GmbH, Mecklenburgische Strasse 27, D-14197 Berlin, Germany

One of the aims of modern microscopy is to quantify two-, three-, or even four-dimensional phenomena in biology, medicine, and material sciences. The requirements imposed on software by such data processing are exemplified by the design considerations of the IMAGIC-5 software system. This system includes facilities for multivariate statistical analysis of large data sets, for correlation averaging of two-dimensional crystals, and for three-dimensional reconstruction of macromolecular structures. The molecules may be arranged as two-dimensional crystals, as helices, or as single particles with arbitrary pointgroup symmetry. IMAGIC's novel angular reconstitution approach allows for the rapid determination of three-dimensional structures of uncrystallized molecules to high resolution. The general organization, user interaction strategy, file structure, and extendibility of IMAGIC are discussed and illustrated with some practical examples. © 1996 Academic Press, Inc.

INTRODUCTION

Advanced microscopy without extensive image processing can no longer be imagined. We here focus on problems of three-dimensional (3D) reconstruction of biological macromolecules based on their two-dimensional (2D) electron microscopic (EM) projections. The basic principles of 3D reconstruction from projections (cf. DeRosier and Klug, 1968) and its ap-

plication to the reconstruction of helically organized macromolecular assemblies (DeRosier and Moore, 1970), of icosahedral viruses (Crowther *et al.,* 1970), and of 2D protein crystals (Henderson and Unwin, 1975) were pioneered largely by the group around Aaron Klug at the MRC in Cambridge, England, in the late sixties and early seventies. A different philosophy, that of analyzing isolated biological macromolecules, was pioneered by the group of Walter Hoppe (cf. Hoppe *et al.,* 1974). Much of the present work in quantitative biological electron microscopy can be traced to the foundations laid at that time.

The growing number of two- and three-dimensional analysis techniques and the interactive character of the minicomputer, which appeared in the mid seventies, created a need for a coherent computing environment in which to perform these tasks and to develop new image processing techniques. Various image processing software systems thus were designed (see review: Hegerl, 1992) including our IMAGIC system (Van Heel, 1979; Van Heel and Keegstra, 1981). Since 1981 the IMAGIC system grew from ~22 000 lines to ~500 000 lines of code and went through major revisions associated with its porting to the VMS and UNIX operating systems, its adaptation to the X Windows (X11) standard, and changes in its user-interaction philosophy.

USER PERSPECTIVE

Problem orientation. The IMAGIC system is problem oriented and the questions addressed to the user while solving a problem concern that one task. It is our philosophy to assemble specialized pro-

---

[1] Current address: College of Biological Science, University of Guelph, Guelph Ontario N1G 2W1, Canada.

grams for each more complicated task, since high-level programs allow much better interactive guidance for the user than do image processing command files or scripts.

User interaction. The user experiences the conversational IMAGIC system in an interactive session. IMAGIC command names are long and self-explanatory (such as "CORRELATION-AVERAGING" or "THREED-TEST-IMAGE") and may be abbreviated. The "?" or "HELP" answer to any question will provide the user with additional information specific to that particular question. Well-formulated interactive help is crucial to exploring the possibilities of the programs or as a memory aid and is used frequently even by experienced IMAGIC users. For some very interactive tasks, a visually oriented user interface is more appropriate than a conversational one, and control windows with push buttons, sliders, etc. are used (cf. Fig. 1b).

Default processing. Whenever the user types an answer to a specific question, that answer becomes the default the next time the question is posed. The second time one then starts a command, one need modify only the parameters that one is not satisfied with. The default values are a substantial memory support which help retrace a line of reasoning.

Multiple images. An image file in IMAGIC includes both a header file and a data file (Van Heel and Keegstra, 1981). The file may contain thousands of images and the system treats them as a unit. The command BAND-PASS-FILTER, for example, automatically processes all the images in the file, unless otherwise specified. The user need not formulate explicit loops over the images to be processed.
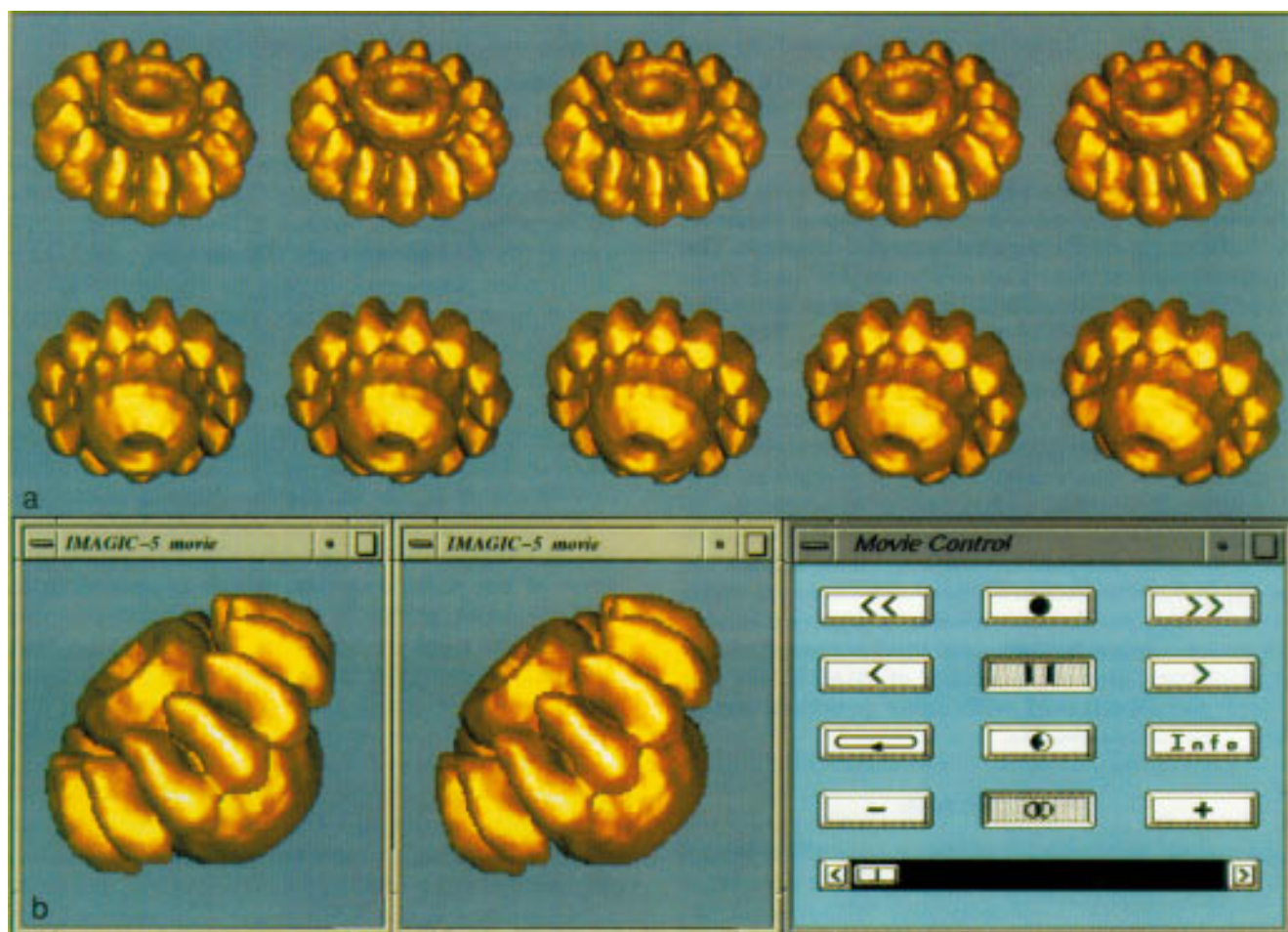

FIG. 1. (a) Continuous stereo surface representation of the ice-embedded portal protein of bacteriophage SPP1. By calculating a sequence of surface-view images with an interimage angle compatible with stereo viewing (about 6°), one can create a continuous stereo representation conveying a good 3D impression even in printed form (Van Heel, 1983). Typically, one will precalculate a full 360° set of images covering a great circle on the unit sphere. Shown here are some contiguous parts of such a great circle set. The portal protein depicted was found to possess an unusual 13-fold rotational symmetry (Dube *et al.,* 1993). (b) By presenting such a great circle sequence of surface representations in rapid succession, one can create the impression of a rotating 3D object. Better still is to present two adjacent movies, whereby the two frames form a pair of stereo images (see illustration). The user can then merge the two images visually (possibly using a stereo viewer) and thus be presented simultaneously with complementary 3D stereoscopic and rotation cues.

Many small programs. The IMAGIC system is a collection of many programs started by the "IMAGIC" supervising program and not a single large entity. Thus, the IMAGIC system is compatible with the basic concepts of the multitasking, X Windows-based workstation. The user may start any number of programs, image display windows, terminals, and plot windows.

Import–export. Many image formats such as "TIFF" and "GIF", used by commercial densitometers and scanners, and various specific formats in use in electron microscopy are accepted as input or output for the IMPORT–EXPORT program. Most "data-only" formats can be made directly accessible to IMAGIC simply by creating a corresponding header file and renaming the data file. The on-the-fly conversion of floating-point data formats allows the use of IMAGIC within mixed-hardware environments.

Educational and testing aspects. IMAGIC can be used to model real data processing runs for educational or testing purposes. Extensive model building facilities allow the user to create all kinds of 2D and 3D data sets. 3D structures may be generated with arbitrary point-group symmetry and may then be repeated into helical aggregates or into 2D crystals with all possible plane groups. The model structures can be projected in various directions, for example, to emulate tilt-series reconstruction experiments in the electron microscope. Noise may be added; images may be randomly rotated and shifted.

TECHNICAL ORGANIZATION

The IMAGIC system, although primarily aimed at analyzing large electron microscopical data sets, is a general purpose floating-point-oriented scientific data analysis system which has been used in such diverse fields as light microscopy, medical positron emission tomography (PET), raster tunneling microscopy (RTM; Haiss *et al.,* 1994), holography (Harscher *et al.,* 1995), Fourier transform infrared spectroscopy (Naumann *et al.,* 1988), and protein sequence analysis (Van Heel, 1991b). Written in the standard languages "FORTRAN" and "C", and adhering to the X11 standard, the system runs on most modern computer systems (AIX, SOLARIS, IRIX, ULTRIX, OpenVMS, OSF/1, etc.). The IMAGIC system is a structured, modular network of programs and routines in which software transparency and maintainability have been optimized. All system-dependent routines are concentrated in a few environment-specific libraries, such as the operating system interface library and the display device interface libraries.

Horizontal and vertical modularity. A vertical modular organization exists in the IMAGIC system to distinguish between the higher levels of software interacting directly with the user and the lower levels of the software interacting with the operating system, the hardware, etc. IMAGIC also has a horizontal modularity referring to programs, libraries, and command definitions which logically belong together. The MSA module, for example, consists of a set of multivariate statistical analysis programs for data compression and classification (see below), the "msalib" library containing specific MSA subroutines, the "msa.icm" command definitions file, and the compilation files needed to install the MSA module on different operating systems. Locally developed programs aimed at performing a given task will also typically be grouped in such a module. A module as a self-contained entity may be transferred and compiled independently into an existing IMAGIC system.

Input/output. An important aspect of the high-volume image processing problems that IMAGIC aims at is the balance between pure calculations and input–output operations to disk. It is not uncommon for an I/O-intensive computer program to exploit only 5–10% of the available CPU capacity because it is continuously waiting for data to be read in from disk, especially when the disk is accessed through a slow and overloaded network. A number of I/O-minimizing strategies are implemented in IMAGIC: a. When opening an IMAGIC image file, a line buffer memory is reserved which may be as large as a full image. Physical I/O operations take place only when the image lines needed are not already in that buffer. b. Small images (up to 512×512 or 768×768 on a 1995 workstation) can be read in once and then be processed by memory-to-memory operations. Extensive in-core processing libraries are implemented and include all single-particle alignment operations. c. The IMAGIC 3D buffering scheme (Borland *et al.,* 1988) allows fast random access within large 3D volumes with limited available memory.

Fast Fourier Transforms. Very important for virtually all processing within the IMAGIC system are Fast Fourier Transforms (FFTs) in one, two, or three dimensions. We use the Singleton mixed-radix FFT algorithm (Singleton 1969) for efficiency. The mixed-radix FFT allows sampling of the data in a problem-oriented way. For example, if the sampling of a 3D volume on a 128^3 grid is insufficient, with a radix-2 algorithm one is forced to migrate to a 256^3 grid representing an eightfold increase in file space and computational requirements, whereas a mixed-radix transform allows one to use a, say, 160^3 grid. Apart from the Singleton FFT algorithm the IMAGIC 2D-FFT and 3D-FFT algorithms are based on the "TRANSPO" algorithm (Van Heel, 1991a), one of the fastest ways of transposing large disk-based multidimensional data sets. The combination of these algorithms allows for the routine calculation

of large multidimensional FFTs, like 1024^2 images or 640^3 volumes.

Extending the system. The IMAGIC system is designed as a development platform for implementing new image processing ideas. Some 10 different "SAMPLE" programs, each containing all necessary IMAGIC infrastructure but differing in buffering philosophy, are available. These programs can be edited to perform new tasks. In-core libraries for the fast processing of small images, and ex-core libraries containing equivalent operations on larger images, can be called from the new programs.

DATA VISUALIZATION

For displaying images and plotting curves IMAGIC relies largely on the X Windows routines. Like all IMAGIC programs, the DISPLAY program by default can loop over all images present in a file to produce galleries of images (Fig. 1a). The first surface rendering programs for the presentation of 3D maps in electron microscopy were developed within IMAGIC (Van Heel, 1983) and were updated to include more elaborate rendering options (Saxton, 1985). An effective procedure for visualizing 3D structures—which can even be used in print—is the continuous stereo sequence (Van Heel, 1983) covering, for example, a great circle of viewing directions around an object. By displaying the images in a gallery such that all left–right neighbors represent stereo pairs, a visual stereo matching of two neighbors causes all pairs in the gallery to match simultaneously (Fig. 1a). Many sets of gradually changing images may be viewed in rapid succession using the MOVIE facility. An appealing option is the displaying of a pair of stereo images, each of which rotates with time (Fig. 1b). This technique is one of the best 3D stereo visualization techniques not requiring special hardware.

ADVANCED METHODS

Multivariate statistical analysis. The MSA approach, which allows the analysis of mixed populations of images, was introduced to electron microscopy some 15 years ago and is now an integral part of many image analysis procedures (Van Heel and Frank, 1980; 1981). With the MSA techniques one considers images as a linear combination of the main eigenvectors ("eigenimages") of the set, thus reducing the total amount of data and facilitating interpretation. The eigenvector analysis was originally performed using the χ^2 metric (Lebart *et al.,* 1984) which is a good metric for histogram data with inherent positivity but is not so good for general signal processing. General signals, including phase-contrast EM images, may have a zero average density, a situation which cannot be dealt with in strict correspondence analysis other than either by adding

a constant or by thresholding the negative densities away. Thus, we now preferably use the modulation metric (Borland and Van Heel, 1990; Van Heel *et al.,* 1992b), although the MSA program allows a flexible choice of metrics.

After the eigenvector eigenvalue data compression, an automatic classification or clustering procedure operating on the compressed data is essential. Our favored approach is the hierarchical ascendant classification scheme (Lebart *et al.,* 1984) in combination with a moving elements postprocessor (Van Heel, 1984a, 1989; Borland and Van Heel, 1990). The eigenvector and classification programs in the MSA module are developed specifically for analyzing very large disk-based data sets (~100 000 molecular images). An important application of MSA techniques is to perform an exhaustive search for "characteristic views" of a molecule present in a mixed population of molecular images (Van Heel and Stöffler-Meilicke, 1985) (Fig. 2). Similar molecular images are averaged into these characteristic views thus strongly reducing the noise in the images (Harauz *et al.,* 1987b; Dube *et al.,* 1993; Serysheva *et al.,* 1995; Schatz *et al.,* 1995).

Alignment techniques. The IMAGIC system has extended facilities for rotational, translational, horizontal, and vertical alignments concentrated in the ALIGN module. These iterative schemes are based on the classical cross-correlation function (CCF) (Steinkilberg and Schramm, 1980) or, alternatively, on the improved mutual correlation function (MCF, Van Heel *et al.,* 1992a). Extensive facilities for multireference alignment (Van Heel and Stöffler-Meilicke, 1985) allow a data set to be aligned with respect to a large set of reference images and are of growing importance in the context of angular reconstitution (see below, and Serysheva *et al.,* 1995). All IMAGIC alignment algorithms calculate the final rotated and shifted image using only a single interpolation step, even when a sequence of translational and rotational alignments have been applied to the images. "Equivalent" rotation and shift parameters are computed throughout the alignment steps thus allowing the calculation of the end results from the input images directly, thus alleviating the loss of resolution entailed by multiple interpolations.

Reference-free alignments and symmetry analysis. Conventional alignments of a set of images with respect to a given reference, however, may bias that data set toward the properties of that reference image (Boekema *et al.,* 1986). To avoid such data bias, a number of approaches have been implemented including: rotationally and translationally invariant function classification (Schatz and Van Heel, 1990, 1992), rotational alignment by classification of translational invariant functions (Van Heel *et al.,* 1992b), and alignment by classification of transla-
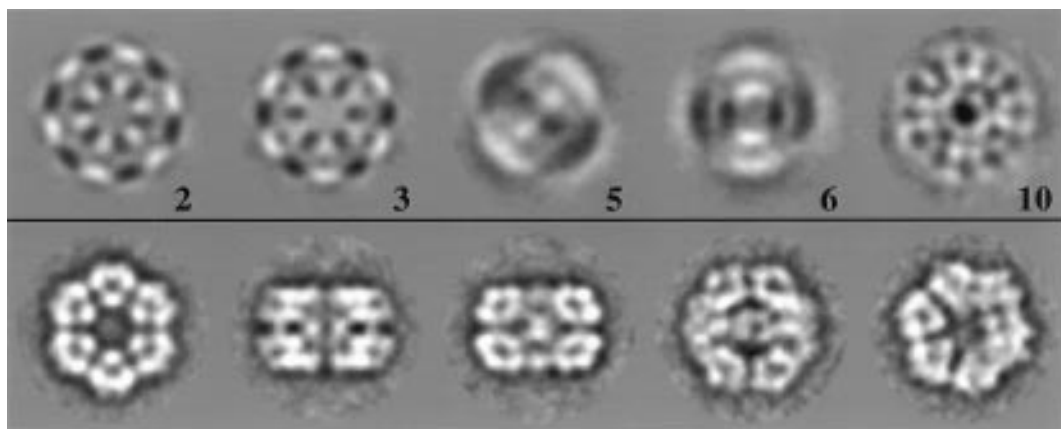
Fig. 2. MSA symmetry analysis of a *Lumbricus terrestris* hemoglobin data set collected from electron images of specimens embedded in vitreous ice. The first step of this analysis encompasses the centering of all molecular images using an iterative translational-only alignment procedure performed with respect to rotationally symmetrized total sums of the data set (Dube *et al.,* 1993). Because of the pointgroup symmetry of the molecule and of the prevalence of specific views, the main symmetry components of the data set emerged directly from the analysis of the full data set. The predominant symmetry property of annelid hemoglobins is sixfold as illustrated by eigenvectors Nos. 2 and 3 (top row) which are "90°" out of phase in a rotational sense. The twofold symmetry axes of this 622 pointgroup symmetric molecule (Royer *et al.,* 1987; Boekema and Van Heel, 1989) are perpendicular to the main sixfold axis and are described by higher eigenvectors (Nos. 5, 6). Our symmetry analysis often serves a double purpose since this "alignment by classification" also is a reference-free and unbiased first step toward finding the characteristic views of a molecule present in a mixed population of images (bottom row; Schatz *et al.,* 1995).

tionally centered molecular images (Dube *et al.,* 1993). The latter approach is, at the same time, a good method for determining the rotational symmetry of a large set of molecular images (Fig. 2) and supersedes the popular rotational power spectrum technique of Crowther and Amos (1971). The use of image moments for reference-free classification of dark-field and electron spectroscopic images has also been implemented and investigated (Beniac and Harauz, 1995).

Correlation averaging. Crystallographic averaging taking imperfections of the crystal into account by "unbending" was one of the first options to be implemented in the IMAGIC system (Van Heel and Hollenberg, 1980). Conventional correlation averaging (Saxton and Baumeister, 1982) can now be used to generate 3D reconstructions of 2D crystallographic specimens (Boekema *et al.,* 1984; Schultz *et al.,* 1993). These procedures, including transferfunction correction, were used to find 2D projection images of porin to ~4 Å resolution (Saß *et al.,* 1989). The newest IMAGIC correlation averaging approach allows the averaging of low-dose high-resolution images of 2D crystals whereby the statistical differences existing between unit cells are taken into account using the MSA classification facilities. These correlation averaging procedures may also exploit the advantages of nonsquared correlation functions like the MCF.

Angular reconstitution. The multireference alignment and MSA classification approaches described above allow us to obtain the various characteristic projections of macromolecules in an EM specimen. However, since these characteristic views are not obtained through any tilting of the specimen holder, we do not *a priori* know what their relative angular orientations are. Early methods for finding these unknown Euler angles (Van Heel, 1984b; Harauz and Van Heel, 1986) led to the development of the angular reconstitution approach (Van Heel, 1987; Goncharov and Gelfand, 1988). Angular reconstitution is based on the common line projection theorem stating that two 2D projections of the same 3D object have at least one (1D) line projection in common. With three or more projections of an asymmetric object, the relative orientation of all projections is fixed.

A number of refinements (Van Heel *et al.,* 1992b; Orlova and Van Heel, 1994; Serysheva *et al.,* 1995; Schatz *et al.,* 1995) of angular reconstitution have rendered the technique one of the most practical and routine techniques for determining the 3D structure of large macromolecular assemblies (Fig. 1). The refinements include a better assignment of Euler angle to a characteristic projection image through the use of "anchor sets" of reprojections, and improvements of the overall alignment of the data set by multi-reference alignment of the full data set with respect to a large set of reprojections covering the asymmetric triangle for the given point-group symmetry (Schatz *et al.,* 1995). Since no tilt-series data collection with multiple exposures of the same specimen area is required, the angular reconstitution technique is simple experimentally. No theoretical upper limit to the resolution attainable by the angular reconstitution technique is in sight. A 3D res-

olution of around 15 Å (in all directions since there is no missing cone) has already been achieved in the case of the *Lumbricus terrestris* hemoglobin (publication in preparation).

Three-dimensional reconstruction. In electron microscopy the first 3D reconstruction schemes were designed for helically arranged polymers (DeRosier and Moore, 1970) and icosahedral viruses (Crowther *et al.,* 1970) and were implemented in Fourier space using polar coordinates. For 3D reconstructions from tilt series of 2D crystals (Henderson and Unwin, 1975; Henderson *et al.,* 1986; Kühlbrandt and Wang, 1991) methods are used which are based on techniques originally developed for X-ray crystallography.

In the IMAGIC system the main current 3D reconstruction algorithm is the exact filter back-projection algorithm (Harauz and Van Heel, 1986; Radermacher, 1988). In filtered back-projection techniques, the Fourier space filtering is generally performed using an analytical filter. This filter is implicitly based on the *a priori* assumption that an infinite number of 2D projections of the 3D structure is available and that their projection directions are uniformly distributed over all possible angles (Harauz and Van Heel, 1986). For the exact filter algorithm, in contrast, a unique filter is applied to each of the 2D projections taking into account the explicit Fourier space overlap between all available projections. The algorithm was first used to solve very large single-tilt-axis 3D reconstructions of a human chromosome (Harauz *et al.,* 1987a; Borland *et al.,* 1988). Our general-geometry algorithm can deal with all possible reconstruction geometries, including the conventional tomography geometry.

DISCUSSION

Hardware developments. In the last 20 years, the speed of computing has increased 1000-fold, while the market cost of data storage on magnetic disks has decreased by as much. As a consequence, computer hardware considerations have shifted to the background and software considerations have come to the foreground. Ten years ago manufacturers offered image processing systems based on special hardware to achieve a high processing throughput for specific tasks. The speed of processing with standard workstation computers has now increased so much that general purpose computers running flexible software, written in portable high-level languages such as FORTRAN and C, often surpass the earlier hard-wired solutions.

Software continuity. The short lifespan of any computer hardware, and thus of software oriented toward that hardware, highlights the continuity aspects of image processing projects which typically run over much longer time scales. In this light it is noteworthy that the image processing software systems in use 15 years ago are still the main systems today (Hegerl, 1992). Many projects are run by doctoral students and continuity is endangered when the students leave the labs. The software tools created in the course of a project must be generated in a systematic way so they are overviewable by the next generation of students. Developing the software in a structured environment like IMAGIC helps in consolidating know-how. Maintenance and continuity of software have become at least as important as the maintenance of the microscope itself. We have found it difficult to achieve long-term continuity in a strictly academic environment, and thus in 1990 decided to commercialize the IMAGIC system.

Current and future developments. One of the most active corners of the IMAGIC system is the "ANGREC" module, containing all the angular reconstitution programs. This module is being used extensively to determine 3D structures of symmetric particles such as the (622 symmetric) *L. terrestris* hemoglobin (Schatz *et al.,* 1995), the (222) *Limulus polyphemus* hemocyanin (Van Heel *et al.,* 1994), the (52) keyhole limpet hemocyanin (Dube *et al.,* 1995), the portal protein structures with 13-fold rotational symmetry (Fig. 1, and Dube *et al.,* 1993), the 4-fold symmetric Ca^{2+}-release channel (Serysheva *et al.,* 1995), and for asymmetric particles such as the *Escherichia coli* ribosome (Stark *et al.,* 1995). The programs are formulated in a Cartesian coordinate system and work for all pointgroup symmetries. With our new approach one may relax the symmetry requirements and thus, for example, analyze an icosahedral virus (532) using only 5, 52, 32, or 222 pointgroup symmetry. The angular reconstitution approach is a flexible tool for studying structure–function relations in biology without crystallizing the protein. In cases where crystals do exist that are suitable for high-resolution X-ray crystallography, the low-resolution (10–30 Å) EM map of the oligomer may help find the high-resolution phases of the X-ray diffraction pattern, a technique currently being explored with the giant hemoglobin of *L. terrestris* (Royer *et al.,* 1987).

A unique development that is taking place in our system is the unification of the reconstruction techniques for specific macromolecular organizations into a single framework. Whereas earlier reconstruction programs were designed specifically for helically arranged polymers (DeRosier and Moore, 1970) or icosahedral viruses (Crowther *et al.,* 1970), the programs in IMAGIC are formulated for the general case. An icosahedral virus is a "single particle" with 532 pointgroup symmetry and a helical fiber is a "single particle" that repeats itself infinitely in one direction. All that is required to analyze helical as-
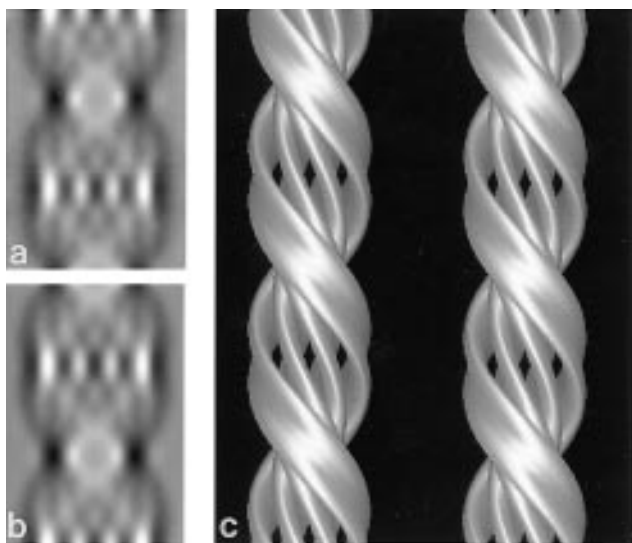
FIG. 3. 3D reconstruction of a helical fiber. Many biological macromolecules can arrange into long helical aggregates so that a single projection image suffices to calculate the 3D reconstruction of the assembly. Within one electron image taken from a direction perpendicular to the axis, we encounter all possible projection images of the repeating unit representing a complete tomographic set of 2D projections of the 3D helical object. The object shown here is a helical aggregate of simple amphiphilic molecule (*N*-octyl-D-gluconamide: Boettcher *et al.,* 1995) which assembles spontaneously when a solution of this molecule is cooled to below its transition temperature of 68°C. The noise-free repeating unit of this fiber is found using alignments and MSA classifications. The reprojection (b) of the 3D reconstruction (c) of the fiber is virtually indistinguishable from the 2D average (a) used to reconstruct the fiber. The intriguing 3D structure consists of a multilayered stack of bilayers twisted into a left-handed helix, a novel supraorganization for amphiphilic molecules.

semblies with the single-particle programs is a consistent approach on reinterpolating the data such that the linear repeats in the helical assembly synchronize with the sampling raster and frame used for processing (Fig. 3). By the same token, a 2D crystal is a "single particle" that repeats itself in two directions. The unification of these approaches, using Cartesian coordinates, contributes considerably to the ease-of-use and ease-of-maintenance of these powerful structure analysis techniques.

REFERENCES

Beniac, D. R., and Harauz, G. (1995) Remarkable moments in single particle electron image analysis, *Optik* **99,** 62–74.

Boekema, E. J., Van Heel, M., and Van Bruggen, E. F. J. (1984) Three dimensional structure of NADH ubiquinone oxidoreductase of the mitochondrial respiratory chain, *Biochim. Biophys. Acta* **787,** 19–26.

Boekema, E. J., Berden, J. A., and Van Heel, M. (1986) Structure of mitochondrial F$_1$-ATPase studied by electron microscopy and image processing, *Biochim. Biophys. Acta* **851,** 353–360.

Boekema, E. J., and Van Heel, M. (1989) Molecular shape of *L. terrestris* erythrocruorin studied by electron microscopy and image analysis, *Biochim. Biophys. Acta* **957,** 370–379.

Boettcher, C., Stark, H., and van Heel, M. (1995) Stacked bilayer helices: A new structural organization of amphiphilic molecules, *Ultramicroscopy,* in press.

Borland, L., Harauz, G., Bahr, G., and Van Heel, M. (1988) Packing of the 30 nm chromatin fiber in the human metaphase chromosome, *Chromosoma* **97,** 159–163.

Borland, L., and Van Heel, M. (1990) Classification of image data in conjugate representation spaces, *J. Opt. Soc. Am.* **A7,** 601–610.

Crowther, R. A., Amos, L. A., Finch, J. T., DeRosier, D. J., and Klug, A. (1970) Three-dimensional reconstruction of spherical viruses by Fourier synthesis from electron micrographs, *Nature* **226,** 421–425.

Crowther, R. A., and Amos, L. A. (1971) Harmonic analysis of electron microscopical images with rotational symmetry, *J. Mol. Biol.* **60,** 123–130.

DeRosier, D. J., and Klug, A. (1968) Reconstruction of three-dimensional structures from electron micrographs, *Nature* **217,** 130–134.

DeRosier, D. J., and Moore, P. B. (1970) Reconstruction of three-dimensional images from electron micrographs of structures with helical symmetry, *J. Mol. Biol.* **52,** 355–369.

Dube, P., Tavares, P., Lurz, R., and Van Heel, M. (1993) Bacteriophage SPP1 portal protein: A DNA pump with 13-fold symmetry, *EMBO J.* **12,** 1303–1309.

Dube, P., Harris, J. R., Orlova, E. V., Zemlin, F., van Heel, M., and Markl, J. (1995) Three-dimensional structure of the keyhole limpet hemocyanin by cryoelectron microscopy and angular reconstitution, *J. Struct. Biol.* **115,** 226–232.

Goncharov, A. B., and Gelfand, M. S. (1988) Determination of mutual orientation of identical particles from their projections by the moments method, *Ultramicroscopy* **25,** 317–328.

Haiss, W., Saß, J. K., Lakey, D., and Van Heel, M. (1994) Analysis and interpretation of STM-images in an electrochemical environment: Copper on Au(111), *in* Cohen, S. (Ed.), Atomic Force Microscopy/Scanning Tunneling Microscopy, pp. 423–436, Plenum, New York.

Harauz, G., and Van Heel, M. (1986) Direct 3D reconstruction from projections with initially unknown angles, *in* Gelsema, E. S., and Kanal, L. N. (Eds.), Pattern Recognition in Practice II, pp. 279–288, North-Holland, Amsterdam.

Harauz, G., and Van Heel, M. (1986) Exact filters for general geometry three dimensional reconstruction, *Optik* **73,** 146–156.

Harauz, G., Borland, L., Bahr, G. F., Zeitler, E., and Van Heel, M. (1987a) Three-dimensional reconstruction of a human metaphase chromosome from electron micrographs, *Chromosoma* **95,** 366–374.

Harauz, G., Stöffler-Meilicke, M., and Van Heel, M. (1987b) Characteristic views of prokaryotic 50S ribosomal subunits, *J. Mol. Evol.* **26,** 347–357.

Harscher, A., Lang, G., and Lichte, H. (1995) Interpretable resolution of 0.2 nm at 100 kV using electron holography, *Ultramicroscopy* **58,** 79–86.

Hegerl, R. (1992) A survey of electron image processing packages, *Ultramicroscopy* **46,** 417–423.

Henderson, R., and Unwin, P. N. T. (1975) Three-dimensional model of purple-membrane obtained by electron microscopy, *Nature* **257,** 28–32.

Henderson, R., Baldwin, J. M., Downing, K. H., Lepault, J., and Zemlin, F. (1986) Structure of purple membrane from *Halobacterium halobium:* Recording, measurement and evaluation of

electron micrographs at 3.5Å resolution, *Ultramicroscopy* **19,** 147–178.

Hoppe, W., Gaßmann, J., Hunsmann, N., Schramm, H. J., and Sturm, M. (1974) Three-dimensional reconstruction of individual negatively stained yeast fatty acid synthetase molecules from tilt-series in the electron microscope, *Hoppe-Seyler's Z. Physiol. Chem.* **355,** 1483–1487.

Kühlbrandt, W., and Wang, D. N. (1991) Three-dimensional structure of plant light harvesting complex determined by electron crystallography, *Nature* **350,** 130–134.

Lebart, L., Morineau, A., and Warnick, K. M. (1984) Multivariate Descriptive Statistical Analysis, Wiley, New York.

Naumann, D., Fijala, V., and Labischinski, H. (1988) The differentiation and identification of pathogenic bacteria using FT-IR and multivariate statistical analysis, *Mikroch. Acta* **I,** 373–377.

Orlova, E. V., and Van Heel, M. (1994) Angular reconstitution of macromolecules with arbitrary point-group symmetry, *in* Jouffrey, B., and Colliex. C. (Eds.), Proceedings of the 13th Int. Cong. on EM, Vol. 1, pp. 507–508, Les Editions de Physique, Les Ulis.

Radermacher, M. (1988) Three-dimensional reconstruction of single particles from random and nonrandom tilt series, *J. Electron Miscrosc. Tech.* **9,** 359–394.

Royer, W. E., Hendrickson, W. A., and Love, W. E. (1987) Crystals of *Lumbricus terrestris* erythrocruorin, *J. Mol. Biol.* **197,** 149–153.

Saß, H. J., Beckmann, E., Büldt, G., Dorset, D., Rosenbusch, J. P., Van Heel, M., Zeitler, E., Zemlin, F., and Massalski, A. (1989) Densely packed β-structure at the protein-lipid interface of porin is revealed by high-resolution cryo-electron microscopy, *J. Mol. Biol.* **209,** 171–175.

Saxton, W. O. (1985) Computer generation of shaded images of solids and surfaces, *Ultramicroscopy* **16,** 387–394.

Saxton, W. O., and Baumeister, W. (1982) The correlation averaging of a regularly arranged bacterial cell envelope protein, *J. Microsc.* **127,** 127–138.

Schatz, M., and Van Heel, M. (1990) Invariant classification of molecular views in electron micrographs, *Ultramicroscopy* **32,** 255–264.

Schatz, M., and Van Heel, M. (1992) Invariant recognition of molecular projections in vitreous ice preparations, *Ultramicroscopy* **45,** 15–22.

Schatz, M., Orlova, E. V., Dube, P., Jäger, J., and Van Heel, M. (1995) Structure of *Lumbricus terrestris* hemoglobin at 30 Å resolution determined using angular reconstitution, *J. Struct. Biol.* **114,** 28–40.

Schultz, P., Celia, H., Riva, M., Sentenac, A., and Oudet, P. (1993) Three-dimensional model of yeast RNA polymerase I determined by electron microscopy of two-dimensional crystals, *EMBO J.* **12,** 2601–2607.

Serysheva, I., Orlova, E. V., Sherman, M., Chiu, W., Hamilton, S., and Van Heel, M. (1995) The skeletal muscle calcium-release channel in its closed state visualized by electron cryomicroscopy and angular reconstitution, *Nature Struct. Biol.* **2,** 18–24.

Singleton, R. C. (1969) An algorithm for computing the mixed radix fast Fourier transform, *IEEE Trans. Audio Electroacoust.* **AU-17,** 294–304.

Stark, H., Mueller, F., Orlova, E. V., Schatz, M., Dube, P., Erdemir, T., Zemlin, F., Brimacombe, R., and Van Heel, M. (1995)

The 70s *E. coli* ribosome at 23Å resolution: Fitting the ribosomal RNA, *Structure* **3,** 815–821.

Steinkilberg, M., and Schramm, H. J. (1980) Eine verbesserte Drehkorrelationsmethode für die Strukturbestimmung biologischer Macromoleküle durch Mittelung elektronenmikroskopischer Bilder, *Hoppe-Seyler's Z. Physiol. Chem.* **361,** 1363–1369.

Unser, M., Trus, B. L., and Steven, A. C. (1989) Normalization procedures and factorial representations for classification of correlation-aligned images: a comparative study, *Ultramicroscopy* **30,** 299–310.

Van Heel, M. (1979) IMAGIC and its results, *Ultramicroscopy* **4,** 117.

Van Heel, M., and Frank, J. (1980) Classification of particles in noisy electron micrographs using correspondence analysis, *in* Gelsema, L. S., and Kanal, L., (Eds.), Pattern Recognition in Practice I, pp. 235–243, North-Holland, Amsterdam.

Van Heel, M., and Hollenberg, J. (1980) The stretching of distorted images of two dimensional crystals, *in* Baumeister, W. (Eds.), Proceedings in Life Sciences: Electron Microscopy at Molecular Dimensions, pp. 256–260, Springer-Verlag, Berlin.

Van Heel, M., and Keegstra, W. (1981) IMAGIC: A fast flexible and friendly image analysis software system, *Ultramicroscopy* **7,** 113–130.

Van Heel, M., and Frank, J. (1981) Use of multivariate statistics in analyzing the images of biological macromolecules, *Ultramicroscopy* **6,** 187–194.

Van Heel, M. (1983) Stereographic representation of three dimensional density distributions, *Ultramicroscopy* **11,** 307–314.

Van Heel, M. (1984a) Multivariate statistical classification of noisy images (randomly oriented biological macromolecules), *Ultramicroscopy* **13,** 165–183.

Van Heel, M. (1984b) Three-dimensional reconstructions from projections with unknown angular relationship, Proc. 8th Eur. Cong. on EM, Vol. 2, pp. 1347–1348, Budapest.

Van Heel, M., and Stöffler-Meilicke, M. (1985) The characteristic views of *E. coli* and *B. stearothermophilus* 30S ribosomal subunits in the electron microscope, *EMBO J.* **4,** 2389–2395.

Van Heel, M. (1987) Angular reconstitution: A posteriori assignment of projection directions for 3D reconstruction, *Ultramicroscopy* **21,** 111–124.

Van Heel, M. (1989) Classification of very large electron microscopical image data sets, *Optik* **82,** 114–126.

Van Heel, M. (1991a) Fast transposing of large multi-dimensional image data sets, *Ultramicroscopy* **28,** 75–84.

Van Heel, M. (1991b) A new family of powerful multivariate statistical sequence analysis techniques, *J. Mol. Biol.* **220,** 877–887 (see also: Taylor, W. (1991) News and views: Spinning in Hyperspace, *Nature* **353,** 388–389).

Van Heel, M., Schatz, M., and Orlova, E. V. (1992a) Correlation functions revisited, *Ultramicroscopy* **46,** 304–316.

Van Heel, M., Winkler, H.-P., Orlova, E. V., and Schatz, M. (1992b) Structure analysis of ice-embedded single particles, *Scanning Microsc.* Suppl. **6,** 23–42.

Van Heel, M., Dube, P., Jäger, J., and Orlova, E. V. (1994) Three-dimensional structure of *Limulus polyphemus* hemocyanin, *in* Jouffrey, B., and Colliex, C. (Eds.), Proceedings of the 13th Int. Congr. on EM, Vol. 3a, pp. 555–556, Les Editions de Physique, Les Ulis.